INTERNATIONAL JOURNAL OF CLIMATOLOGY
Int. J. Climatol. (2011)
Published online in Wiley Online Library
(wileyonlinelibrary.com) DOI: 10.1002/joc.2304

RMetS
Royal Meteorological Society

Interannual variations of tropical cyclone activity over the north Indian Ocean

Eric K. W. Ng and Johnny C. L. Chan*
Guy Carpenter Asia-Pacific Climate Impact Centre, School of Energy and Environment, City University of Hong Kong

ABSTRACT: An examination of the interannual variations of tropical cyclone (TC) activity over the North Indian Ocean during 1983–2008 has been carried out. The results suggest that instead of local sea surface temperatures, such variations, at least over the Bay of Bengal (BB) during October-November-December (OND), can be attributed to similar variations in the atmospheric flow patterns and moist static energy that are apparently forced largely by the El Niño/Southern Oscillation (ENSO). In an El Niño year, conditions for TC genesis and development, including 850-hPa relative vorticity, 200–850-hPa vertical shear of zonal wind, moist static energy, 500-hPa zonal wind, 500-hPa and 850-hPa geopotential height and 200-hPa divergence, are generally less favourable in BB and fewer intense cyclones are observed during OND. The reverse occurs during a La Niña event. However, causes of the variability of TC activity over BB during April-May-June and that over Arabian Sea have yet to be found, which may be due to the small sample size. Copyright © 2011 Royal Meteorological Society

KEY WORDS interannual variability; tropical cyclones; north Indian Ocean

Received 26 July 2010; Accepted 24 January 2011

1. Introduction

In the past few years, claims have been made that the power dissipation (2005) and the number of intense hurricanes and typhoons (Webster *et al*., 2005) have been on the increase, which is likely to be associated with an increase in sea surface temperature (SST) due to global warming. However, earlier studies by Wang and Chan (2002), and Chan and Liu (2004, hereafter, CL04) found no relationship between the locations of tropical cyclone (TC) formation and *in situ* SST anomalies in the western North Pacific (WNP). CL04 also obtained a slightly negative correlation between SST and accumulated cyclone energy (ACE, Bell *et al*., 2000) over the WNP, but no significant relationship can be identified between local SST and average typhoon activity. These results suggested that other than thermodynamic factors, the dynamic factors should not be neglected, which was the conclusion of Chan (2009). Chan (2007) extended the CL04 study to identify the possible causes of the interannual variations of intense typhoon activity over the WNP by investigating the relationship of SST and other meteorological variables with ACE. He found that instead of SST, a large percentage of the variations is related to the planetary-scale atmospheric circulation and thermodynamic structure caused by the El Niño/Southern Oscillation (ENSO) phenomenon.

For the north Indian Ocean (NIO), Danard and Murty (1989), and Yu and Wang (2009), respectively, found increasing TC frequency and potential intensity in a doubled-CO_2 world. On the other hand, observational studies identified a significant declining trend in TC (depression or above) frequency during the monsoon seasons over either northern Bay of Bengal (BB) (Rajeevan *et al*., 2000) or the entire BB (Patwardhan and Bhalme 2001; Rajendra Kumar and Dash, 2001; Jadhav and Munot, 2009) in spite of increasing SST in recent decades. Xavier and Joseph (2000) suggested a possible dependence of this recent decreasing TC frequency on vertical wind shear. Mandake and Bhide (2003) extended the study to show a possible link between atmospheric parameters and the decreasing TC frequency since 1980. Dash *et al*., (2004) also discussed the weakening of favourable parameters for TC formation in recent years. Pattanaik (2005) analysed both oceanic and atmospheric parameters during high- and low-frequency periods of TC occurrence and similar to Chan (2007), concluded that the variability of large-scale atmospheric circulation, instead of SST, is the main cause of variability in TC activity. These observational studies generally focused only on the TC frequency and mostly on the interdecadal variability of TC activity. The TC intensity and the interannual variability of TC activity, which are equally important, have not been examined in detail. Even though Singh *et al*. (2000, 2001) made an effort to examine the trend of intense TC activity to represent TC intensity, only the frequency of these TCs has been studied instead of employing a quantifiable parameter, such as ACE.

* Correspondence to: Johnny C. L. Chan, School of Energy and Environment, City University of Hong Kong, Tat Chee Ave., Kowloon, Hong Kong, China. E-mail: Johnny.Chan@cityu.edu.hk

This study is therefore an attempt to examine systematically the interannual variations of TC activity (both intensity and frequency) over the NIO and their possible relationship between local SST and other parameters. Section 2 describes the data and methodology used. Section 3 reveals the variability and periodicity of TC parameters. Section 4 analyses the possible relationship between TC parameters and local SSTs. The impact of large-scale parameters on TC activity is then studied in Section 5. The paper is concluded in Section 6, with suggestions on future studies.

2. Data and methodology

2.1. TC data

The data of TCs over the NIO are extracted from the International Best Track Archive for Climate Stewardship (IBTrACS) Project website (http://www.ncdc.noaa.gov/oa/ibtracs/). Several parameters are defined in this study: (1) number of TCs (NTC), comprises all TCs contained in the IBTrACS data (maximum sustained wind speed $\geq$25 knots), so as to increase the sample size; (2) number of intense cyclones (NIC) (maximum sustained wind speed $\geq$64 knots); (3) ACE, defined as 10^{-4} times the sum of square of a intense cyclone's maximum speed (v_{max}, but only for time periods when the maximum sustained wind speed is 35 knots or higher) for each 6-h period of its existence, i.e. $ACE = 10^{-4} \sum v_{max}^2$.

Unlike CL04, the ratio of NIC to NTC is not studied, as the TC activity over the NIO is not as active as that over the WNP, especially over the Arabian Sea (AS) where no TCs occurred in some years.

Owing to the absence of meteorological satellite over the NIO (see http://www.isro.org/), only data from 1983 to 2008 are analysed. The month and year of each TC is assigned as the time first recorded in the IBTrACS dataset. Because the development characteristics over BB and AS are different (Gray 1968), investigation is carried out separately for BB and AS in this study. Some results of the entire NIO are also shown for reference. The TCs are labelled as from BB or AS according to their origin, i.e. according to their positions first recorded in the IBTrACS dataset.

2.2. SST data

The SST data are from the Extended Reconstructed SST data set V3b of the National Oceanic and Atmospheric Administration (NOAA). The horizontal resolution of the dataset is 2° latitude × 2° longitude. Generally, TCs over the NIO reach their maximum intensity south of 25 °N and east of 50 °E (Figure 1). The SST within the domain 5°–25 °N, 50°–100 °E is therefore considered. The SST of BB and AS are selected to be within the domain 5°–25 °N, 80°–100 °E (hereafter BB local SST) and 5°–25 °N, 50°–80 °E (hereafter AS local SST), respectively.

2.3. Atmospheric data

The atmospheric data are from the reanalyses of the US National Centers for Environmental Prediction/National Center for Atmospheric Research (http://www.esrl.noaa.gov/psd/data/gridded/data.ncep.reanalysis.html). The horizontal resolution of the dataset is 2.5° latitude × 2.5° longitude.

2.4. The Nino 3.4 index and Indian Ocean dipole mode index (DMI)

The NOAA Climate Prediction Center Nino 3.4 Index is extracted from the website of the NOAA Earth System Research Laboratory (http://www.esrl.noaa.gov/psd/data/climateindices/list/), while the DMI is from the website of Japan Agency for Marine-Earth Science and Technology (http://www.jamstec.go.jp/frcgc/research/d1/iod/). Positive Indian Ocean Dipole (IOD) years are defined in which September-October-November (SON) mean DMI are $\geq$0.5, while negative IOD years are with SON mean DMI ≤ -0.5.

For easy comparison, all variables are standardized. All discussions of the various time series are therefore based on standardized values, unless otherwise stated.

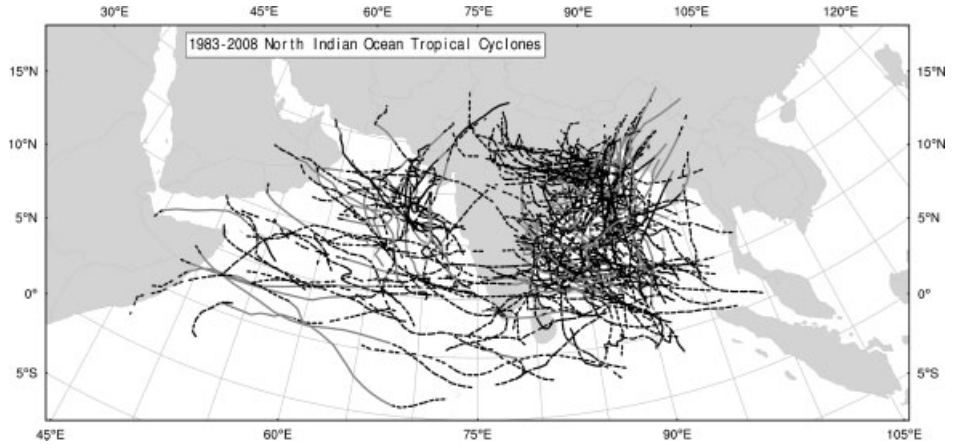

Figure 1. Tracks of TCs over the NIO during 1983–2008, dashed, dark grey, and black tracks indicate maximum wind speed (10-minute) <35 knots, ≥35 knots, and <65 knots, and ≥65 knots, respectively.

3. Interannual variations of TC parameters

3.1. Variability of TC parameters

The time series of annual NTC, NIC, and ACE over BB and AS show significant interannual variation from 1983 to present (Figure 2). For example, the annual ACE over BB attains a peak in 1999 and drops to a minimum in 2001. However, contrary to the projections of numerical models (Danard and Murty, 1989; Yu and Wang, 2009) and previous study (Singh *et al*., 2001), significant increasing trends can only be found for the annual NTC over BB and ACE over AS (>90% confidence level) based on the t-test.

All the TC parameters time series of the entire NIO have very similar variation as those of BB due to the high portion of NIO TC initially formed in BB (Figure 3). Except for AS during October-November-December (OND), when only one intense cyclone (IC) occurred during 1983–2008, the time series of ACE highly correlates with that of NIC during IC seasons (correlation coefficient $R > 0.83$), which is significant at the 99% confidence level. Therefore, due to the small sample size of NIC, the TC intensity in the NIO is studied only by investigating the ACE hereafter. Results from these time series analyses of the TC parameters also confirm Gray's (1968) finding that the development characteristics of TC activity in BB and AS are different.

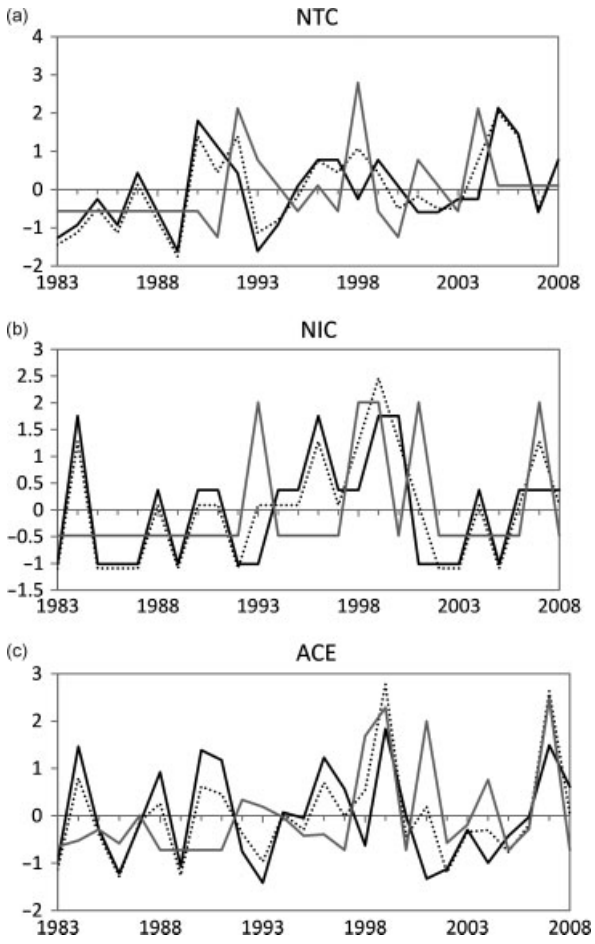

Figure 2. The time series of anomaly of annual (a) NTC, (b) NIC, and (c) ACE over the NIO (dashed), BB (black), and AS (grey) during 1983–2008, respectively.

3.2. Periodicity of TC parameters

The best way to determine the dominant modes of variability and the change of those modes with time is to apply a wavelet analysis to the various time series. The real-valued Mexican hat wavelet (derivate of a Gaussian; $m = 2$) is used. The global wavelet spectrum is chosen as the background spectrum, which is the most appropriate test for non-stationary changes in variance (Kestin *et al*., 1998). More information on wavelet analysis can be found in Torrence and Compo (1998).

The wavelet power spectra (WPS) of NTC over BB shows strongest signals in the 2–7-yr band (Figure 4(a)), while that of ACE has peaks around both the 2–7 and 8–16-yr bands (Figure 4(b)), with the 2–7-yr band being prominent during the early part of the study period and the 8–16-yr band becoming more pronounced since 1997. Over AS, the strongest signal in the WPS for annual NTC is again in the 2–7-yr band (Figure 4(c)) and that for ACE in 2–4 and 5–10-yr, with exceptionally low variance early in the study period (Figure 4(d)). These results suggest that variations in TC frequency and intensity over the NIO may possibly be linked to climatic oscillations, e.g. ENSO or IOD around the 2–8-yr band and 2-yr band respectively (e.g. Trenberth, 1976; Wang and Wang, 1996; Behera and Yamagata, 2003), which has been suggested by Singh *et al*. (2000) for TC frequency and will be investigated further in Section 4.2.

4. Relationship between TC parameters and SSTs

4.1. Coherence between the time series of TC parameters and local SSTs

Given the increasing awareness of global warming, the relationship between TC parameters and local SSTs has been widely discussed recently, as introduced in Section 1. Such a possible relationship for BB and AS is therefore examined in this section using wavelet coherence (WTC).

WTC is used for frequency bands and time intervals identification during which two time series are co-varying. It is especially useful in determining coherence for intervals in which both WPS have minimal power (Torrence and Webster, 1999). On the contrary, without normalising to the single WPS, cross wavelet transform are only appropriate for phase estimation for significant sections (Maraun and Kruths, 2004). The Morlet wavelet is instead used for the wavelet coherence transform.

As all the ICs and over 75% of TCs are found during April-May-June (AMJ) and OND (Figure 3), only TC activities during these two IC seasons are examined. The squared WTC over each region during each season is investigated separately. Except for the BB ACE during OND which shows significant coherence around 2–6-yr band (Figure 5), none of the TC parameters in either AMJ or OND period shows significant relationship in their squared WTCs with the corresponding local SSTs

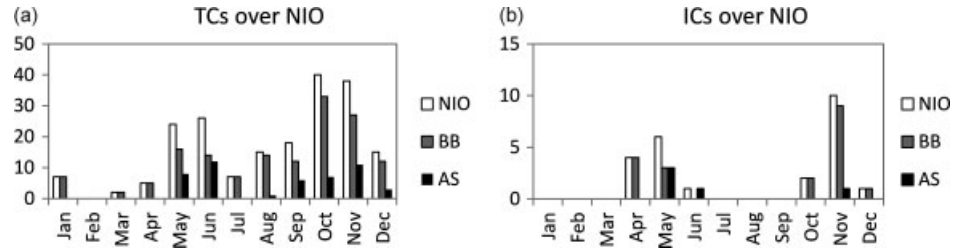

Figure 3. The annual occurrence of (a) TCs and (b) ICs over the entire NIO basin (white), BB (grey), and AS (black) during the period 1983–2008.

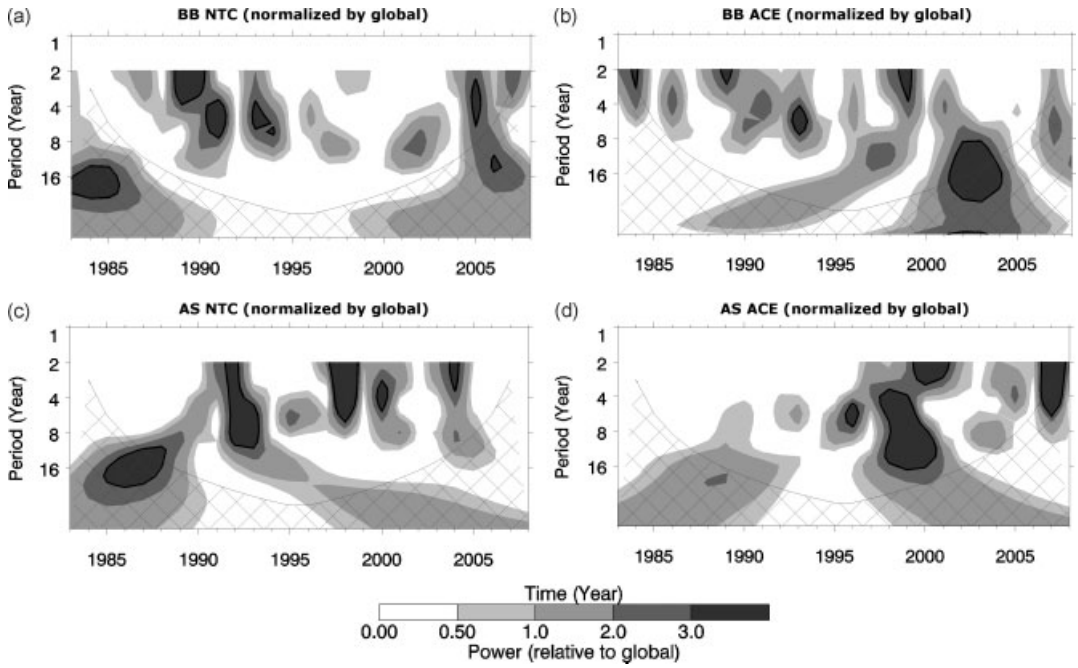

Figure 4. (a) The normalized WPS of annual NTC over BB. The power of WPS has been scaled by the global wavelet spectrum. The cross-hatched region is the cone of influence (COI), where zero padding has reduced the variance. Black contour is the 95% confidence level, using the global wavelet as the background spectrum. (b) Same as (a), except for ACE. (c) Same as (a), except for AS. (d) Same as (a), except for ACE over AS.

(not shown). In other words, only BB local SST may possibly influence the ACE there. On the other hand, although the mean phase angle of $\sim 153^{\circ}$ in Figure 5 shown by the vectors does not seem to be meaningful to this annual OND mean analysis, the slowly varying phase angles not only further confirm the possible relationship between ACE and local SST over BB during OND, but also imply that there may be a phase shift between them. Nevertheless, no significant result can be seen when comparing the time series variation of local SSTs (Figure 6) to that of TC parameters. Further, as the WPS for annual mean local SST over BB and AS also show dominant oscillations in 2–7 and 5–9-yr bands respectively (not shown), TC parameters and local SST may both be linked to climatic oscillations, which is to be discussed in Section 4.2.

4.2. Correlations between TC parameters and climatic oscillations

To identify the possible relationships between climatic oscillations and TC parameters, climatic oscillation indices averaged over AMJ and OND are correlated with TC parameters of the same periods. Significant results are again found only over BB.

Consistent with local SSTs, neither the correlation of the Nino 3.4 index nor DMI with TC parameters during AMJ is significant, while better correlation relationships are found during OND. The TC parameters of BB show significant correlation with Nino 3.4 index and DMI during OND (Table I), while those of AS do not (Table II). BB ACE negatively correlates with Nino 3.4 index. In fact, since 1983 over BB, all El Niño years are associated with below-mean ACE (Table III) and 5 out of 7 La Niña years with above-mean ACE (Table IV), with the mean ACE of El Niño and La Niña years being significantly different at 99%. NTC, on the other hand, shows negative correlation with DMI for BB, but its significant correlation relationship with ENSO as found by Singh *et al*., (2000) cannot be found. However, the possible NTC-IOD relationship over BB cannot be revealed in our 2–7-yr variance time series or WTC analyses (not shown), although similar results can still be found for other relationship

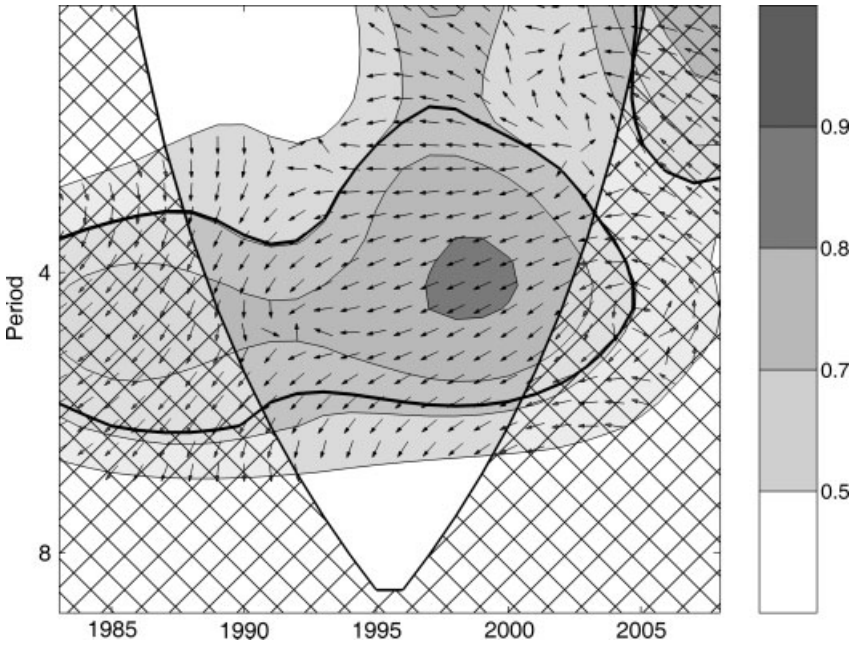

Figure 5. The WTC squared and phase between local SST and ACE over BB during OND. The thick black contour is 95% confidence level against red noise. The cross-hatched region is the COI. The relative phase relationship of significant sections is shown as arrows (with pointing right indicates in-phase and pointing left indicates anti-phase and pointing straight down indicates the lead of local SST by 90°).

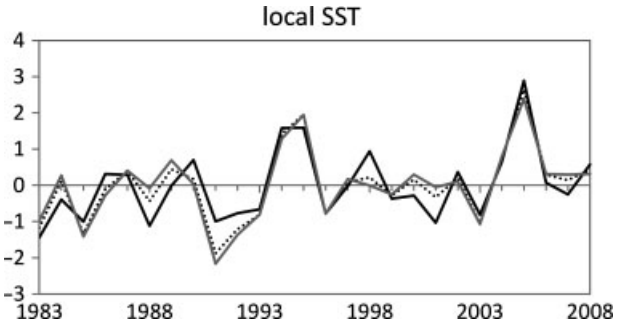

Figure 6. Same as Figure 2(a), except for local SSTs.

between TC parameters and climatic oscillations. Since WTC can identify intermittent correlations, which then helps enhance the linear correlation analyses in the time-frequency space (Gurley and Kareem, 1999; Gurley *et al*., 2003), if two phenomena exhibit significant correlation relationship, significant region should also be shown in their squared WTC, which is not the case for the IOD-NTC relationship. Therefore, the significant linear correlation coefficient between IOD and NTC may be resulted from noises and thus, they do not seem to be related, at least in this study period. This result is different from Singh (2008), which may be due to the short study period used or different definition of TC frequency and suggests that the influence of IOD on BB NTC may result from its decadal variability which cannot be identified from current study period, as Ashok *et al*. (2004) also found significant decadal peaks (8–13 yrs) for IOD.

To summarize, none of the TC parameters shows significant relationship with either ENSO or IOD during

Table I. Correlation coefficients between climatic oscillation and TC parameters over the entire NIO basin (top), BB (middle), and AS (bottom) during the period of OND. Numbers in italic indicate correlations that are statistically significant at the 95% confidence level. Both Nino 3.4 index and DMI are averaged over the period of OND.

	NTC	ACE	NIC
NIO			
Nino 3.4	−0.14	*−0.68*	*−0.60*
DMI	*−0.47*	*−0.48*	*−0.48*
BB			
Nino 3.4	−0.23	*−0.66*	*−0.61*
DMI	*−0.41*	−0.36	*−0.48*
AS			
Nino 3.4	0.13	0.05	0.05
DMI	−0.05	−0.19	−0.03

Table II. Same as Table I, except for AMJ.

	NTC	ACE	NIC
NIO			
Nino 3.4	0.01	−0.04	0.01
DMI	−0.26	*0.41*	*0.42*
BB			
Nino 3.4	0.09	0.13	0.16
DMI	−0.09	0.34	0.34
AS			
Nino 3.4	−0.11	−0.17	−0.18
DMI	−0.37	0.16	0.16

Table III. Variation of tropical cyclone activity parameters in El Niño years over the entire NIO basin (left), BB (center), and AS (right) during OND. Numbers in italics indicate values below the climatological mean (1983–2008).

El Niño year	NTC	NIO ACE(kt^2)	NIC	NTC	BB ACE(kt^2)	NIC	NTC	AS ACE(kt^2)	NIC
1986	*3*	*1.21*	*0*	*2*	*0.57*	*0*	1	0.64	*0*
1987	5	*4.36*	*0*	5	*4.36*	*0*	*0*	*0*	*0*
1991	*3*	*0.57*	*0*	3	*0.57*	*0*	*0*	*0*	*0*
1994	*2*	*3.11*	*0*	*1*	*0.79*	*0*	1	2.32	*0*
1997	*2*	*1.06*	*0*	*1*	*1.06*	*0*	1	*0*	*0*
2002	4	*1.68*	*0*	3	*1.68*	*0*	1	*0*	*0*
2004	5	*3.90*	*0*	*2*	*0*	*0*	2	3.90	*0*
2006	*1*	*0.49*	*0*	*0*	*0*	*0*	1	*0.49*	*0*
Mean	3.13	2.05	0.00	2.13	1.13	0.00	0.88	0.92	0.00
Climatological Mean (83–08)	3.65	5.62	0.50	2.77	4.71	0.46	0.81	0.91	0.04

Table IV. Same as Table III, except for La Niña years. Numbers in italics indicate values above the climatological mean (1983–2008).

La Niña year	NTC	NIO ACE(kt^2)	NIC	NTC	BB ACE(kt^2)	NIC	NTC	AS ACE(kt^2)	NIC
1984	3	*16.34*	*2*	*3*	*16.34*	*2*	0	0	0
1988	*4*	*13.27*	*1*	*4*	*13.27*	*1*	0	0	0
1995	3	*9.15*	*1*	2	*7.76*	*1*	*1*	*1.38*	0
1998	*6*	*5.80*	*1*	*3*	2.79	*1*	*3*	*3.01*	0
1999	3	*18.17*	*2*	*3*	*18.17*	*2*	0	0	0
2000	*4*	*7.51*	*2*	*4*	*7.51*	*2*	0	0	0
2008	*5*	1.54	0	*4*	1.54	0	*1*	0	0
Mean	4.00	10.25	1.29	3.29	9.63	1.29	0.71	0.63	0.00
Climatological Mean (83–08)	3.65	5.62	0.50	2.77	4.71	0.46	0.81	0.91	0.04

AMJ, while ACE during OND appears to be related to ENSO over BB.

4.3. Effect of climatic oscillations on local SSTs

The local SST over BB could be a response to ENSO similar to BB ACE during OND, as its WPS has most of the significant power within the 2–7-yr band (not shown). The impact of ENSO on local SST is hence studied. Here, monthly Nino 3.4 index and local SST data are used to provide more insight into the relationship.

The squared WTC between SST and Nino 3.4 index over BB during OND shows significant monthly and interannual variations (Figure 7). Since our focus is on interannual variation, only that will be discussed. Other than the high coherence in 1-yr band that can be expected due to their strong seasonal variability, significant coherence can be found in 2–7-yr band, which is agreed to be the dominant band of ENSO. The vectors indicate a lag of BB local SST by 45°. This is reasonable as BB local SST reaches peak during summer and Nino 3.4 during December-January-February. These results suggest a strong relationship between BB local SST and ENSO. To better study the influence of local SST on BB ACE during OND, partial wavelet squared coherence (PWC) is necessary to remove the ENSO effect on BB local SST during OND.

4.4. Wavelet coherence and phase between TC parameters and local SSTs after removal of ENSO effects

WTC works like traditional correlation coefficient and it thus can be thought as a localized correlation coefficient in time-frequency space (Grinsted *et al*., 2004). Following this, Mihanović *et al*. (2009) suggested calculating the squared PWC to eliminate the influence of the effect of a time series $x2_n$ from the relationship of the two time series, y_n and $x1_n$, squared PWC $(RP_n^{YX1\_X2})^2$ is defined from R_n^{YX1}, R_n^{YX2} and R_n^{X2X1}, which are the WTC between y_n and $x1_n$; y_n and $x2_n$; $x1_n$ and $x2_n$ respectively, as:

$$(RP_n^{YX1\_X2})^2 = \frac{|R_n^{YX1} - R_n^{YX2} \cdot R_n^{X2X1^*}|^2}{(1-(R_n^{YX1})^2)(1-(R_n^{X2X1})^2)'} \quad (1)$$

where asterisk indicates complex conjugation.

Owing to the relationship between BB local SST and Nino 3.4 index during OND revealed in section 4.3, which suggests that the possible link between BB local SST and BB ACE during OND may be influenced by ENSO effect, PWC is applied to remove the ENSO effect.

After removal of the ENSO effect, the squared PWC between BB local SST and BB ACE during OND indicates notable reduction of the significant sections

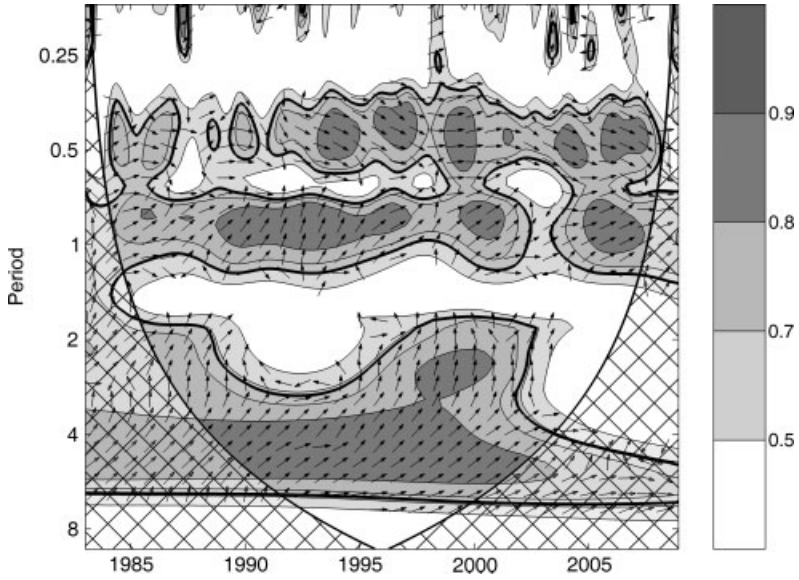

Figure 7. Same as Figure 5, except for monthly local SST over BB and Nino 3.4 index. The relative phase relationship of significant sections is shown as arrows (with pointing right indicates in-phase and pointing left indicates anti-phase and pointing straight down indicates the lead of monthly local SST by 90°).

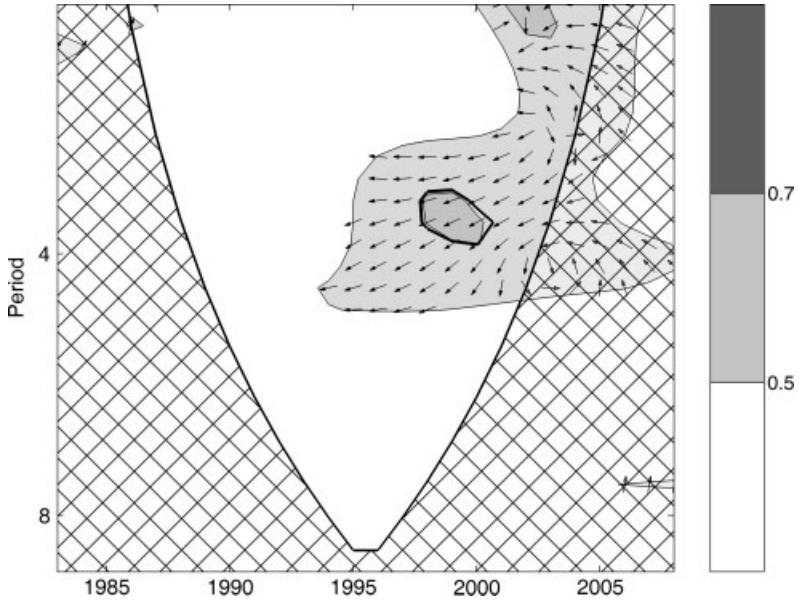

Figure 8. The PWC and phase between BB local SST and BB ACE after removal of ENSO effect during OND. The thick black contour is 95% confidence level against red noise. The cross-hatched region is the COI. The relative phase relationship of significant sections is shown as arrows (with pointing right indicates in-phase and pointing left indicates anti-phase and pointing straight down indicates the lead of BB local SST by 90°).

(Figure 8), providing evidence for the significant contribution of ENSO effect on the BB SST-ACE relationship. The significant areas originally shown in squared WTC almost completely disappear after the removal of ENSO effect. Therefore, BB ACE during OND apparently does not vary in response to the increasing local SST over BB. Consistent results can also be found in linear correlations coefficients and partial correlation maps (not shown).

In summary, local SST over BB and AS does not have a significant direct effect on TC parameters of the corresponding region, but rather forced by the ENSO event through alternation of the atmospheric circulation. This is consistent with CL04 over WNP and will be further studied in Section 5.

5. Impact of large-scale parameters on TC activity

Gray (1979) proposed 6 large-scale parameters that likely govern TC genesis and development, including three dynamic factors: Coriolis parameter, low-level (850-hPa) relative vorticity and vertical shear of the horizontal wind; and three thermodynamic factors: mid-level moisture, moist instability of the low- to mid-level (500-hPa)

atmosphere and SST with oceanic mixed layer. Akin to CL04 and following Goh and Chan (2010) that referred to previous studies on favourable factors on TC formation and intensification (e.g. Ho *et al*., 2004; Liu and Chan, 2008; Yumoto and Matsuura, 2001), the impacts of 7 parameters, including 850-hPa relative vorticity (850RV), 200−850-hPa vertical shear of zonal wind (VS), moist static energy (MSE), 500-hPa zonal wind (500U), 500-hPa, and 850-hPa geopotential height (500H and 800H), and 200-hPa divergence (DIV), on TC activity are explored by applying empirical orthogonal function (EOF) analysis via correlation matrices. The signs of EOFs are chosen to give negative correlation with ENSO and IOD.

As in Section 4, the two seasons AMJ and OND are separately investigated by first averaging the large-scale parameters in each period. Standardisation is applied to the time series of annual mean large-scale parameters of individual grid points before EOF analysis is implemented. Correlations are then computed for the time coefficients of each mode, respectively, with TC parameters and climatic oscillation indices. Lastly, a stepwise regression analysis is performed on these time coefficients to identify the dominant modes statistically among those having a high correlation with TC parameters.

Of all the principal components, significant correlations over 95% confidence level with the time series of the principal components of large-scale parameters are mostly found for TC parameters over BB during OND. The few significant correlations found over AS during both AMJ and OND, and BB during AMJ may be due to the small sample size, which is the drawback of using the data only during the period with satellite observations. Hence, with more significant results, discussions are made only for the modes during OND that reveal significant correlations with TC parameters over BB.

5.1. 850-hPa relative vorticity

The first EOF (EOF1) of 850RV of OND shows interannual low-level relative vorticity variation from far eastern BB to western AS, explaining 24.2% of total variance (Figure 9). Maximum amplitude is found east of ∼68 °E, which indicates largest interannual low-level relative vorticity variation at that region.

The corresponding time series of this PC (PC1) reveals positive correlations with that of BB NTC and ACE, with correlation coefficients R of 0.46 and 0.42 respectively, significant at 98 and 95% confidence level. The positive correlations suggest that strong low-level relative vorticity favours both TC frequency and intensity, which is consistent with CL04 and agrees with previous studies (e.g. Lee *et al*., 1989; Briegel and Frank, 1997). Besides, this time series is significantly correlated with Nino 3.4 index and DMI at 99% confidence level, values of R being −0.63 and −0.71, respectively, which implies that weaker (stronger) low-level relative vorticity can be observed during an El Niño (La Niña) year or a positive (negative) IOD year.

5.2. 200-hPa divergence

The EOF1 of DIV does not show significant correlation with TC parameters and will not be discussed here. The second EOF (EOF2) shows a sandwich-like pattern (Figure 10) that explains 14.8% of total variance, revealing a negative maximum west of ∼65 °E and a positive one east of ∼80 °E, in which the largest interannual variation of DIV can be found.

The R between this PC (PC2) and that of NTC is 0.48, which is significant at 98% confidence level. This result suggests that strong outflow due to DIV is favourable to TC formation, which has also been found by Yumoto and Matsuura (2001) for WNP. Furthermore, PC2 is significantly correlated with Nino 3.4 index and DMI at 95 and 99% confidence level respectively (R being −0.41 and −0.76, respectively). This result signifies that DIV is relatively weaker (stronger) during an El Niño (La Niña) year or a positive (negative) IOD year.

5.3. 500-hPa geopotential height

Since the EOF1 and EOF2 of 500H are highly correlated with ACE and NTC respectively, they will both be discussed later on. While the EOF1 represents 67.0% of the total variance and shows positive signs over the entire domain (not shown), EOF2 explains 19.5% of total variance and exhibits a south-north dipole (Figure 11).

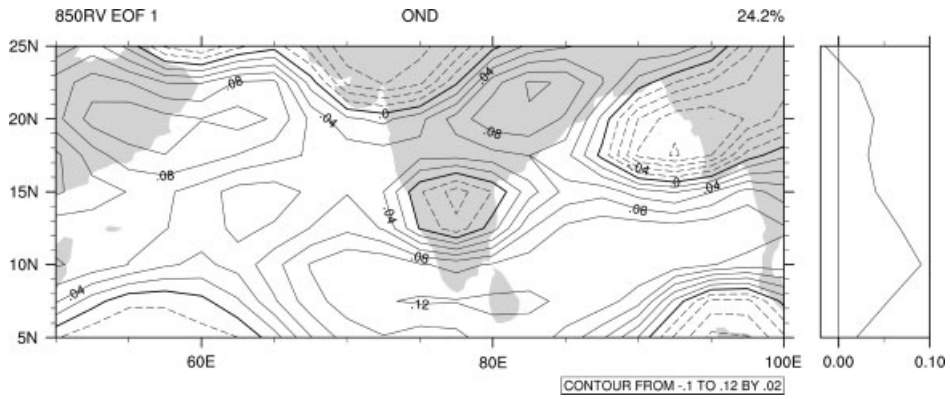

Figure 9. EOF1 of the annual mean OND 850RV, where the sign of the EOF is chosen so that it is negatively correlated with Nino 3.4 index and DMI.

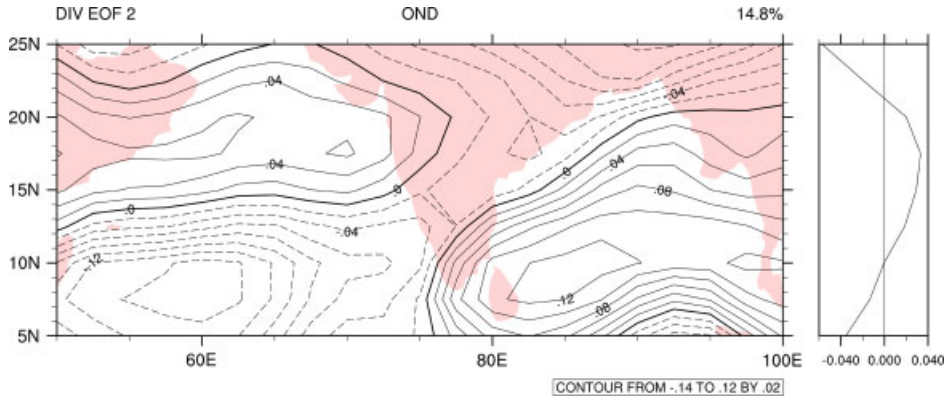

Figure 10. Same as Figure 9, except for DIV EOF2. This figure is available in colour online at wileyonlinelibrary.com/journal/joc

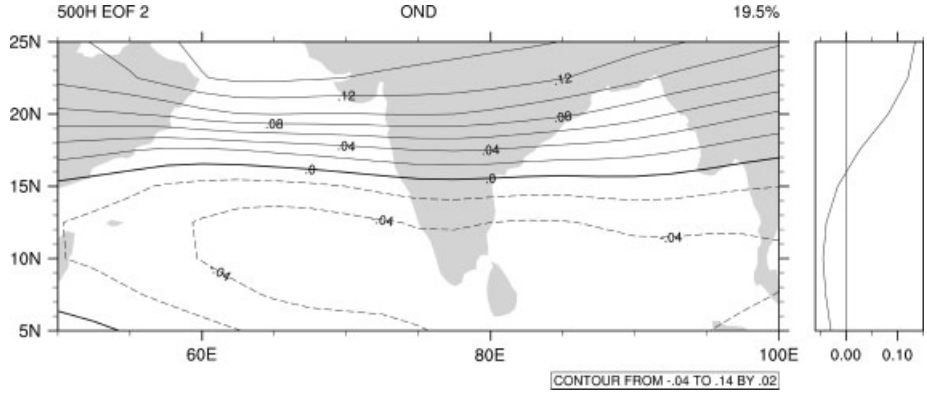

Figure 11. Same as Figure 9, except for 500H EOF2.

The time series of PC1 and PC2 of 500H are positively correlated with ACE and NTC respectively, which is significant at 99 and 95% confidence level accordingly ($R = 0.56$ and $R = 0.39$, respectively). Higher 500H will therefore lead to more TC activity, which is also suggested by previous studies (e.g. Ho *et al.*, 2004). The PC1 is correlated well with Nino 3.4 index and DMI at 99% confidence level ($R = -0.64$ and $R = -0.67$, respectively) and PC2 with Nino 3.4 index at 95% confidence level ($R = -0.43$). That is, lower (higher) 500H can be found during an El Niño (La Niña) year or a positive (negative) IOD year.

5.4. Moist static energy and 500-hPa zonal wind

Both the EOF2 of MSE (pressure-weighted mean over 1000–500 hPa layer) and EOF1 500U indicate a dipole pattern, with that of MSE appears like a southwest-northeast one and 500U a south-north one (Fig. 12 and Fig. 13). The EOF2 of MSE interprets 24.5% of total variance, whereas the EOF1 of 500U clarified 51.8%. Again, regions with maximum amplitudes exhibit greatest interannual variation of either MSE or 500U there.

The time series of PC2 of MSE and PC1 of 500U are found to have positive correlation with NTC which are both significant at 98% confidence level (Rs of 0.56 and 0.49 respectively). These results infer that higher MSE value and stronger 500U will result in more TC formation only. The PCs are also significantly correlated with Nino 3.4 index and IOD ($R < -0.46$; >95% confidence level). In other words, less (more) MSE and weaker (stronger) 500U is associated with El Niño (La Niña) year or a positive (negative) IOD year.

5.5. Vertical shear of the zonal wind and 850-hPa geopotential height

The EOF1s of VS and 850H reveal negative signs consistently over the entire domain (not shown). While the EOF1 of VS illustrates the variability of westerly and easterly shear over the NIO that describes 71.3% of total variance, that of 850H explains 75.0% of total variance for the variability of the geopotential height at 850-hPa.

As positive correlations can be found between the PC1 of VS and 850H and TC parameters ($R > 0.44$; >95% confidence level) and PC1s have significant correlation relationship with Nino 3.4 index and DMI ($R < -0.57$; >99% confidence level), these results signify the relationship of TC activity to vertical wind shear over the NIO found by Xavier and Joseph (2000) and high geopotential height at 850-hPa over the WNP emphasized by Liu and Chan (2008), and imply that during an El Niño (La Niña) year or a positive (negative) IOD year, anomalous westerly (easterly) shear and lower (higher) 850H can generally be seen.

Noted, that although the correlation maps of the PCs of the seven factors reveal some regions having significant correlation relationships with TC parameters and

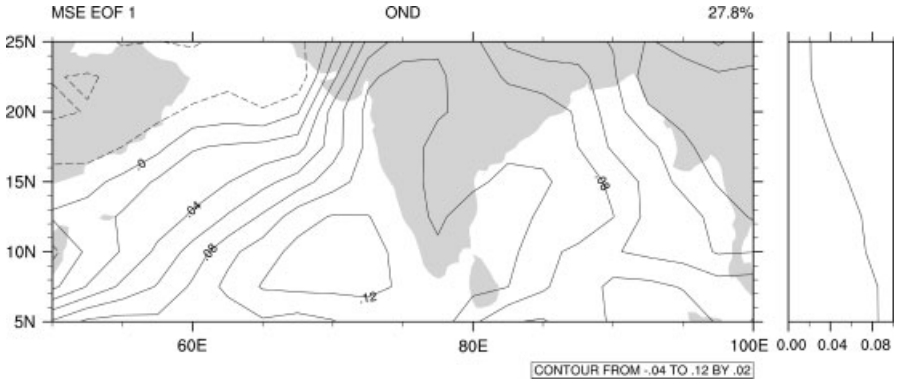

Figure 12. Same as Figure 9, except for MSE.

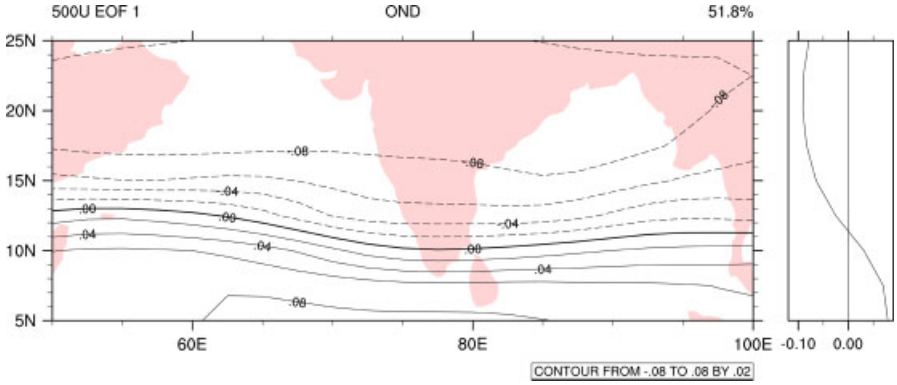

Figure 13. Same as Figure 9, except for 500U. This figure is available in colour online at wileyonlinelibrary.com/journal/joc

local SST over the NIO, the corresponding partial correlation maps after the removal of ENSO effect (not shown) show great reduction in both magnitude and the area extent of correlation pattern. This result further confirms the contribution of ENSO to the interannual variation of the 850RV, VS, MSE, 500U, 500H, 800H, and DIV, and the unlikely forcing of local SST on TC activity. It is also consistent with CL04 and further concluded by Chan (2009) that except for the Atlantic, SST may only act as a necessary condition for TC intensification and dynamic factors should rather be considered as sufficient conditions.

5.6. Dominant modes of BB TC activity during OND

With backward stepwise regression analysis, dominant modes are selected statistically based on their contribution, with the linear regression equations for TC parameters over BB during OND given as:

$$NTC = 2.769 - 0.6371 \times VS_1 + 0.4187 \times DIV_2; \quad (2)$$

$$ACE = 4.711 + 1.833 \times 500H_1 + 2.407 \times 850H_1, \quad (3)$$

where the subscript number following each factors indicate the EOF, 1 for EOF1 and 2 for EOF2.

Therefore, during OND over BB, NTC is strongly related to EOF1 of VS and EOF2 of MSE (multiple $R = 0.59$; $>99\%$ confidence level), while ACE has totally different dominant modes, including EOF1 of 500H and 850H (multiple $R = 0.67$; $>99\%$ confidence level). Much consideration should be put on these factors when establishing models for TC predictions.

5.7. Summary

The impact of seven large-scale dynamic and thermodynamic factors, including 850RV, VS, MSE, 500U, 500H, 800H, and DIV, on NIO TC activity has been studied with EOF analysis and dominant factors are selected statistically respectively for NTC and ACE using stepwise linear regression. Significant correlations are found mostly over BB during OND between TC parameters and the PCs of large-scale parameters and less significant results are found over AS during both AMJ and OND, and over BB during AMJ, which may be due to the small sample size. Results found that during an El Niño (La Niña) year, weaker (stronger) low-level relative vorticity, anomalous westerly (easterly) shear, less (more) MSE, weaker (stronger) 500U, lower(higher) 500H and 800H, and weaker (stronger) DIV, at least for BB during OND, could be observed. ENSO therefore has a significant impact on these large-scale parameters, which provides less (more) favourable conditions for TC genesis and development in an El Niño (La Niña) year. Although significant correlations are found between DMI and PC1s of large-scale parameters, DMI does not correlate well with TC parameters and only Nino 3.4 shows significant

correlation with BB ACE. Thus, only BB ACE can be said to be forced by ENSO. Consistent with CL04 and Chan (2009), it may be concluded that dynamic factors, constrained by ENSO effect are likely the main cause of TC variability, instead of SST.

6. Discussion and conclusion

The present study uses a similar approach as that of Chan and Liu (2004) to study systematically the interannual variation of tropical cyclone (TC) activity (both intensity and frequency) over the north Indian Ocean (NIO) and their possible relationship between local sea surface temperature (SST) and other parameters during 1983–2008. Significant interannual variations have been found for the annual mean time series of the three TC parameters, including the number of TCs (NTC), number of intense cyclones (NIC) and accumulated cyclone energy (ACE). However, except for the annual NTC over Bay of Bengal (BB) and ACE over Arabian Sea (AS), no significant increasing trend of NTC and ACE can be found within the study period. The wavelet power spectra suggest that the variation of TC activity may be related to climatic oscillations. In particular, BB ACE is found to have dominant oscillations around 2–7 and 8–16-yr bands, which is shown to be forced by the ENSO during October-November-December (OND). Wavelet coherence and partial wavelet coherence (after the removal of ENSO effect) reveal no significant relationship between SST and TC parameters, which is consistent with previous studies (e.g. Rajeevan *et al*., 2000; Chan and Liu, 2004) and contradicts with results suggested by many numerical climate models. By means of the alternation of the large-scale circulation, El Niño/Southern Oscillation (ENSO) phenomenon indeed forces the interannual variation of BB TC activity during OND, while the exact factors leading to interannual variability of TC activities over AS for either April-May-June (AMJ) or OND have yet to be found. Impact of large-scale parameters on TC activity has been explored by empirical orthogonal function (EOF), in which meaningful results are found mostly over BB during OND. Weaker low-level relative vorticity, anomalous westerly shear, less moist static energy, weaker 500-hPa zonal wind, lower 500 and 850-hPa geopotential height and weaker 200-hPa divergence, at least for BB during OND, can be observed during an El Niño year, which provide less favourable conditions for TC genesis and development. Less TC activity is thus observed in an El Niño year during OND over BB. The reverse occurs during a La Niña year. With stepwise regression, EOF1 of 200–850-hPa vertical shear of zonal wind and EOF2 of moist static energy, and EOF1 of geopotential height of 500 and 850-hPa are respectively selected statistically as the dominant modes leading to the variability of BB NTC and ACE during OND. Nevertheless, the causes leading to the variability of TC activity over BB during AMJ and that over AS cannot be found, which may be due to the small sample size.

Despite no significant correlations found between Indian Ocean Dipole (IOD) and TC parameters, the Indian Ocean Dipole Mode Index (DMI) is significantly correlated with PCs of large-scale parameters during OND that are in turn correlated well with TC parameters. Although a high correlation has been found between the Nino 3.4 index and DMI, previous studies suggested that IOD is unlikely to be a part of ENSO phenomenon (Saji *et al*., 1999; Saji and Yamagata, 2003a, b) and Ashok *et al*. (2001) found IOD weakening the relationship between Indian summer monsoon rainfall and ENSO. We could therefore expect IOD may also affect the relationship between TC activity and ENSO by influencing the large-scale parameters, which then either enhance or weaken the favourable conditions for TC genesis and development. Since ENSO is a stronger oscillation, which may have overridden the effect of weaker IOD, it is reasonable that the correlations of DMI with TC parameter may not be as significant as that of Nino 3.4 index. A study on the individual and combined influence of ENSO and IOD, similar to Ashok and Guan (2004) for the summer monsoon, should therefore be conducted for BB TC activity during OND in the future. Furthermore, Chen and Tam (2010) pointed out that the geographical location of the Nino 3.4 region may possibly mix up the impact of conventional ENSO and that of the recently found ENSO Modoki (Ashok *et al*., 2007) and discussed the effect of ENSO Modoki on TC activity over the western North Pacific. Therefore, a further study should also be carried out to study separately the impact of two types of ENSO events on the TC activity over the NIO. Investigation could also be extended to examine the variation of large-scale parameters and their contribution to cyclogenesis and development during monsoon months, which may lead to the lower TC or IC frequency during those months, i.e. double peak in annual TC activity over the NIO. However, difficulties arise when studying TC activity over the NIO, especially over AS where only a few TCs occur in one year. The investigation in this paper should be revisited when more reliable records from metrological satellite are available.

In conclusion, instead of local SSTs, the interannual variation of TC activity, at least over BB during OND, can be attributed to the variation in the atmospheric dynamic and thermodynamic conditions that largely forced by ENSO effect. Consistent with Chan (2009), the results of present paper also suggest that local SST may only be a necessary but not sufficient condition, while dynamic factors are likely sufficient conditions for TC intensification, and should not be neglected in investigations of seasonal TC activity.

Acknowledgments

Special thanks to T. W. Kowk for his help in developing software of partial wavelet coherence http://www.cityu.edu.hk/gcacic/wavelet and W. Zhou for her valuable advice. Wavelet software was provided by C. Torrence and G. Compo while software package for cross

wavelet transform and wavelet coherence was provided by G. Aslak, and is available at the URL: www.pol.ac.uk/home/resaerch/waveletcoherence.

References

Ashok K, Guan Z. 2004. Individual and combined influences of ENSO and the Indian Ocean Dipole on the Indian summer monsoon. *Journal of Climatologuy* **17**: 3141–3155.

Ashok K, Guan Z, Yamagata T. 2001. Impact of the Indian Ocean Dipole on the relationship between the Indian Monsoon rainfall and ENSO. *Geophysical Research Letters* **30**: 1821, DOI:10.1029/2003GL017926.

Ashok K, Chan WL, Motoi T, Yamagata T. 2004. Decadal variability of the Indian Ocean dipole. *Geophysical Research Letters* **31**: L24207, DOI:10.1029/2004GL021345.

Ashok K, Behera SK, Rao SA, Weng H, Yamagata T. 2007. El Niño Modoki and its possible teleconnection. *Journal of Geophysical Research* **112**: C1107, DOI:10.1029/2006JC003798.

Behera SK, Yamagata T. 2003. Influence of the Indian Ocean Dipole on the Southern Oscillation. *Journal of the Meteorological Society of Japan* **81**: 169–177.

Bell GD, Halpert MS, Schnell RC, Higgins W, Lawrimore J, Kousky VE, Tinker R, Thiaw W, Chelliah M, Artusa A. 2000. Climate assessment for 1999. *Bulletin of the Amererican Meteorological Society* **81**: S1–S50.

Breigel LM, Frank WM. 1997. Large-scale influences on tropical cyclogenesis in the western North Pacific. *Monthly Weather Review* **125**: 1397–1413.

Chan JCL. 2007. Interannual variations of intense typhoon activity. *Tellus* **59A**: 455–460.

Chan JCL. 2009. Thermodynamic control on the climate of intense tropical cyclones. *Proceedings of the Royal Societyof London Series A* **495**: 3011–3021.

Chan JCL, Liu KS. 2004. Global warming and western North Pacific typhoon activity from an observational perspective. *Journal of Climate* **17**: 4590–4602.

Chen G, Tam T-Y. 2010. Different impact of two kinds of Pacific Ocean warming on tropical cyclone frequency over the western North Pacific. *Geophysical Research Letters* **37**: L01803, DOI:10.1029/2009GL041708.

Danard M, Murty TS. 1989. Tropical cyclones in the Bay of Bengal and CO_2 warming. *Natural Hazards* **2**: 387–390.

Dash SK, Jenamani RK, Shekhar S. 2004. On the decreasing frequency of monsoon depressions over the Indian region. *Current Science* **86**(10): 1406–1411.

Emanuel KA. 2005. Increasing destructiveness of tropical cyclones over the past 30 years. *Nature* **436**: 686–688.

Goh AZC, Chan JCL. 2010. Interannual and interdecadal variations of tropical cyclone activity in the South China Sea. *International Journal of Climatology* **30**: 827–842.

Gray WM. 1968. Global view of the origin of tropical disturbances and storms. *Monthly Weather Review* **96**: 669–700.

Gray WM. 1979. Hurricanes: Their formation, structure, and likely role in the tropical circulation. In *Meteorology over the Tropical Oceans*, Shaw DB (ed.), Royal Meteorological Society: Bracknell, UK; 155–218.

Grinsted A, Moore JC, Jevrejeva S. 2004. Application of the cross wavelet transform and wavelet coherence to geophysical time series. *Nonlinear Processes in Geophysics* **11**: 561–566.

Gurley K, Kareem A. 1999. Application of wavelet transforms in earthquake, wind and ocean engineering. *Engineering Structures* **21**: 149–167.

Gurley K, Kijewski T, Kareem A. 2003. First- and higher-order correlation detection using wavelet transforms. *Journal of Engineering Mechanics* **129**: 188–201.

Ho CH, Baik JJ, Kim JH, Gong DY, Sui CH. 2004. Interdecadal changes in summertime typhoon tracks. *Journal of Climate* **17**: 1767–1776.

Jadhav SK, Munot AA. 2009. Warming SST of Bay of Bengal and decrease in formation of cyclonic disturbances over the Indian region during southwest monsoon season. *Theoretical and Applied Climatology* **96**(3): 327–336.

Kestin TS, Karoly DJ, Yano J-I, Rayner NA. 1998. Time-frequency variability of ENSO and stochastic simulations. *Journal of Climate* **11**: 2258–2272.

Lee CS, Edson R, Gray WM. 1989. Some Large-scale characteristics associated with tropical cyclone development in the North Indian Ocean during FGGE. *Monthly Weather Review* **117**: 407–426.

Liu KS, Chan JCL. 2008. Interdecadal Variability of Western North Pacific Tropical Cyclone Track. *Journal of Climate* **21**: 4464–4476.

Mandake SK, Bhide UV. 2003. A study of decreasing storm frequency over Bay of Bengal. *Journal of the Indian Geophysical Union* **7**(2): 53–58.

Maraun D, Kruths J. 2004. Cross wavelet analysis: significance testing and pitfalls. *Nonlinear Processes in Geophysics* **11**: 505–514.

Mihanović H, Orlić M, Pasrić Z. 2009. Diurnal thermocline oscillations driven by tidal flow around an island in the Middle Adriatic. *Journal of Marine Systems* **78**: S157–S168.

Pattanaik DR. 2005. Variability of oceanic and atmospheric conditions during active and inactive periods of storms over the Indian region. *International Journal of Climatology* **25**: 1523–1530.

Patwardhan SK, Bhalme HN. 2001. A study of cyclonic disturbances over India and the adjacent oceans. *International Journal of Climatology* **21**: 527–534.

Rajeevan M, De US, Prasad RK. 2000. Decadal variation of sea surface temperatures, cloudiness and monsoon depressions in the north Indian Ocean. *Current Science* **79**(3): 283–285.

Rajendra Kumar J, Dash SK. 2001. Interdecadal variations of characteristics of monsoon disturbances and their epochal relationships with rainfall and other tropical features, *International Journal of Climatology* **21**(6): 759–771.

Saji NH, Yamagata T. 2003a. Structure of SST and surface wind variability during Indian Ocean Dipole Mode Events: COADS observations. *Journal of Climate* **16**: 2735–2751.

Saji NH, Yamagata T. 2003b. Possible impacts of Indian Ocean Dipole mode events on global climate. *Climate Research* **25**: 151–169.

Saji NH, Goswami BN, Vinayachandra PN, Yamagata T. 1999. A dipole mode in the tropical Indian Ocean. *Nature* **401**: 360–363.

Singh OP. 2008. Indian Ocean Dipole mode and tropical cyclone frequency. *Current Science* **94**(1): 29–31.

Singh OP, Khan TMA, Rahman MS. 2000. Changes in the frequency of tropical cyclones over the North Indian Ocean. *Meteorology and Atmospheric Physics* **75**: 11–20.

Singh OP, Khan TMA, Rahman MS. 2001. Has the frequency of intense tropical cyclones increased in the north Indian Ocean? *Current Science* **80**(4): 575–580.

Trenberth KE. 1976. Spatial and temporal variations of the Southern Oscillation. *Quarterly Journal of the Royal Meteorological Society* **102**: 639–653.

Torrence C, Compo GP. 1998. A practical guide to wavelet analysis. *Bulletin of the American Meteorological Society* **79**: 61–78.

Torrence C, Webster PJ. 1999. Interdecadal changes in the ENSO-monsoon system. *Journal of Climate* **12**: 2679–2690.

Wang B, Chan JCL. 2002. How Strong ENSO Events Affect Tropical Storm Activity over the Western North Pacific. *Journal of Climate* **15**: 1643–1658.

Wang B, Wang Y. 1996. Temporal structure of the Southern Oscillation as revealed by waveform and wavelet analysis. *Journal of Climate* **9**: 1586–1598.

Webster PJ, Holland GJ, Curry JA, Chang H-R. 2005. Changes in tropical cyclone number, duration, and intensity in a warming environment. *Science* **309**: 1844–1846.

Xavier PK, Joseph PV. 2000. Vertical wind shear in relation to frequency of monsoon depressions and tropical cyclones of Indian Seas. *Proc. TROPMET-2000, National Symp. On Ocean and Atmosphere,* Cochin, India, Indian Meteorological Society, 232–245.

Yu J, Wang Y. 2009. Response of tropical cyclone potential intensity over the north Indian Ocean to global warming. *Geophysical Research Letters* **36**: L03709, 5.

Yumoto M, Matsuura T. 2001. Interdecadal variability of tropical cyclone activity in the Western North Pacific. *Journal of the Meteorological Society of Japan* **79**: 23–35.

